Molecular electronics: controlled manipulation, noise and graphene architecture

Tewari, S.

5. Anomalous non-linear shot noise at high voltage bias

Since the work of Walter Schottky, it is known that the shot-noise power for a completely uncorrelated set of electrons increases linearly with the time averaged current. At zero temperature and in the absence of inelastic scattering the linearity relation between noise power and average current still holds even for correlated electrons. Through high-bias shot-noise measurements on single Au atom point contacts, we find that the noise power in the high-bias regime shows highly non-linear behavior even leading to a decrease in shot noise with voltage. We explain this non-linearity using a model based on quantum interference of electron waves with varying path difference due to scattering from randomly distributed defect sites in the leads, which makes the transmission probability for these electrons both energy and voltage dependent.

5.1 Introduction

It is known from the time Walter Schottky in 1918[1], that the noise power increases linearly with time averaged current $S_{\text{Poisson}} = 2e\langle I\rangle$. In mesoscopic devices, where the Pauli's exclusion principle introduces correlations among the electrons, the shot noise drops below this S_{Poisson} value[2]. This reduction has been measured experimentally both in 2DEG based point contacts[3,4] and metallic point contacts[5]. Even here, at zero temperature and in the absence of inelastic scattering, shot noise is known to increase linearly with average current (or applied bias), as given by the expression[6–8]

$$S_{\text{I}} = 2\frac{e^2}{h}\left\{4k_B\theta\sum_{n=1}^{N}T_n(E_{\text{F}})^2 + 2eV\coth(\frac{eV}{2k_{\text{B}}\theta})\sum_{n=1}^{N}T_n(E_{\text{F}})(1-T_n(E_{\text{F}}))\right\} \tag{5.1}$$

where θ is the temperature of the point contact and $T_n(E_{\text{F}})$ is the transmission probability of the n^{th} channel involved in the transport, measured at the Fermi energy E_{F} of the leads. Any deviation from this linearity relation has been attributed to interactions with other degrees of freedom, such as inelastic electron-phonon interaction[9], flicker noise, two level fluctuations[10], heating or non-equilibrium occupation of phonons[11]. The conductance of these point contacts is given by the celebrated Landauer's conductance formula[12], which describes conductance as directly proportional to the sum of the transmission probabilities of the channels involved ($G = 2e^2/h\sum T_n(E_{\text{F}})$). This sets an upper limit for the maximum conductance for a single channel taking part in transport, equal to the quantum of conductance ($G_0 = 2e^2/h$).

These properties for noise and differential conductance hold under quasi equilibrium or in the linear regime, where the transmission probability (T) of a channel is taken as constant, equal to its value at the Fermi energy (E_{F}). In general, the transmission probability of a channel can have both energy and voltage dependence $T(E,V)$. This could bring new pleasant surprises and could also upset current views based on the linear regime. Thanks to a newly developed setup[13] we are able to measure noise continuously as a function of bias, up to very high bias, where the T cannot be taken as constant and the energy and voltage dependence of T gives rise to highly non-linear behavior in shot noise. The non-linearity of shot noise with applied bias can be so strong that it can even lead to negative differential shot noise (NDSN). To understand these non-linearities we use a model based on quantum interference of

[1] W. Schottky. In: *Annalen der Physik* 362 (1918), p. 541.
[2] G. B. Lesovik. In: *JETP Lett.* 49 (1989), p. 592.
[3] M. Reznikov et al. In: *Phys. Rev. Lett.* 75 (1995), p. 3340.
[4] A. Kumar et al. In: *Phys. Rev. Lett.* 76 (1996), p. 2778.
[5] H. E. van den Brom and J. M. van Ruitenbeek. In: *Phys. Rev. Lett.* 82 (1999), p. 1526.
[6] C. W. J. Beenakker and H. van Houten. In: *Phys. Rev. B* 43 (1991), p. 12066.
[7] Th. Martin and R. Landauer. In: *Phys. Rev. B* 45 (1992), p. 1742.
[8] M. Büttiker. In: *Phys. Rev. B* 46 (1992), p. 12485.
[9] Manohar Kumar et al. In: *Phys. Rev. Lett.* 108 (2012), p. 146602.
[10] Ruoyu Chen et al. In: *Phys. Rev. B* 85 (2012), p. 235455.
[11] D. F. Urban et al. In: *Phys. Rev. B* 82 (2010), p. 121414.
[12] R. Landauer. In: *IBM Journal of Research and Development* 32 (1988), p. 306.
[13] Sumit Tewari et al. In: *Review of Scientific Instruments* 88 (2017), p. 093903.

electron waves which take varying paths while being scattered from randomly distributed defect sites in the leads in combination with the usual scattering at the point contact. This quantum interference model leads to energy and voltage dependence of T and explains various types of experimental noise measurements recorded at high bias.

5.2 Measurement setup

High-bias shot-noise measurements are challenging as 1/f noise or flicker noise increases with the square of the applied bias and so at high bias one is likely to be confronted with a large 1/f noise background over the desired shot noise. This forces us to perform measurements at high frequencies where the 1/f noise decreases. We have developed a new high-frequency shot-noise measurement setup described in chapter 4, which can measure noise in the MHz frequency range and can record the spectral information. This spectral information can be recorded with high speed up to 12 spectra/s. This system is connected to a mechanically controlled break junction setup to study shot noise in metallic point contacts and single-molecule junctions with a high mechanical stability. A schematic of the setup is shown in Figure 5.1.

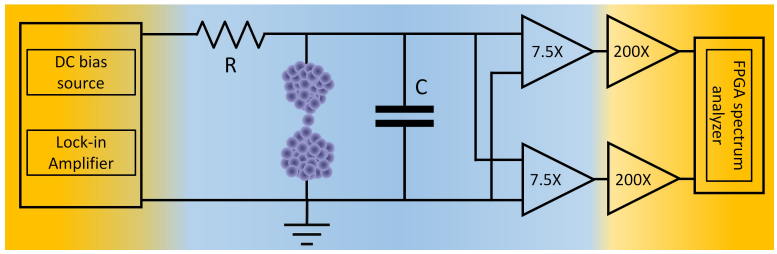

Figure 5.1: Schematic of the experimental setup. The color gradient shows qualitatively the operating temperature from 300 K (orange) to 4.2 K (blue). The setup consists of a cryogenic (7.5X) and room temperature amplifier (200X) together giving 1500 times amplification. The decoupling resistor R is 10 kΩ and the total stray input capacitance at the cryogenic amplifier is around 14 pF.

5.3 Shot-noise measurements

Ballistic single atom point contacts formed between metallic leads have been an important playground to study electronic transport in nano-structures. Both conductance and shot-noise measurements of these contacts have led researchers to understand interesting atomic-scale physics. We start by showing the low-bias shot-noise data, where the usual linear-regime behavior is expected. Figure 5.2(a) shows the linearly increasing shot-noise power as we ramp the voltage bias over a metallic point contact. Depending on the strength of the electron-vibron coupling, the electrons could also pass through the contact by inelastically exciting a vibration mode of atoms forming the junction. This opens an additional inelastic channel for the electron transport over the existing elastic channel. This is known to give a kink in the linearly increasing shot-noise power, as shown for a short chain of Au atoms in Figure 5.2 (b) and is also described in previous work by Kumar et al[9].

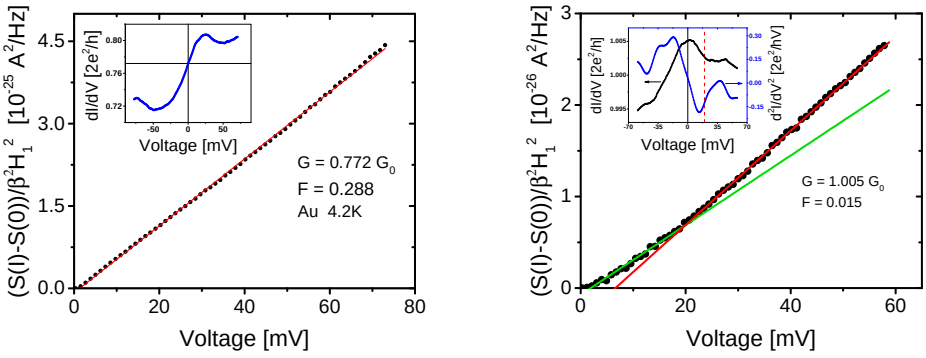

(a) (b)

Figure 5.2: (a) Linearly increasing shot noise with the applied bias over the Au point contact with inset showing the corresponding differential conductance of the contact, (b) Kink in shot noise due to electron phonon interaction close to the vibration mode in Au atomic chain at around 20 meV as seen in the $\mathrm{d}^2I/\mathrm{d}V^2$ shown in the inset

The results shown in Figure 5.2 is what we expect for the linear regime where the transmission is almost constant. But when we go to higher bias and the transmission is close to 1, the shot noise measured over single Au atom point contact shows highly non-linear behavior. A collection of three different examples which we will examine here is shown in Figure 5.3. These point contacts are formed using mechanically controlled break junctions. Differential conductance measurements are performed before and after the noise measurements to verify the stability of the contact. Figure 5.3 shows differential conductance (left) and excess shot noise (S(I)-S(0)) measured (right) for the three cases.

Selected examples shown in Figure 5.3 have differential conductance spectra that are quite different from each other. In example 1 the differential conductance is fairly symmetric and the measured noise (shown with circular points in the right panel of Ex 1) increases linearly at low bias and then it has a kink around 60 mV followed by a further increase up to 325 mV. This kink can not be due to electron-phonon interaction because the Debey energy for Au is around 20 mV. In example 2, the differential conductance is almost anti-symmetric about zero bias and the noise shown in column (b) of Ex 2 shows a different type of non-linearity. Here the noise has a staircase like structure, where the noise stagnates at the middle and rises again. Example 3 has a very strong asymmetry in the differential conductance of the contact accompanied by even stronger non-linearity in the shot noise, showing even a negative differential shot noise i.e., a decrease of shot noise with bias. Here the noise is measured up to 800 mV which is much higher than any previous shot-noise measurement done[14,15] over metallic point contacts. At these high-bias levels one would expect the noise measurement to become affected by 1/f noise and two-

[14] Ruoyu Chen et al. In: *Scientific reports* 4 (2014), p. 4221.
[15] Ruoyu Chen and D. Natelson. In: *Nanotechnology* 27 (2016), p. 245201.

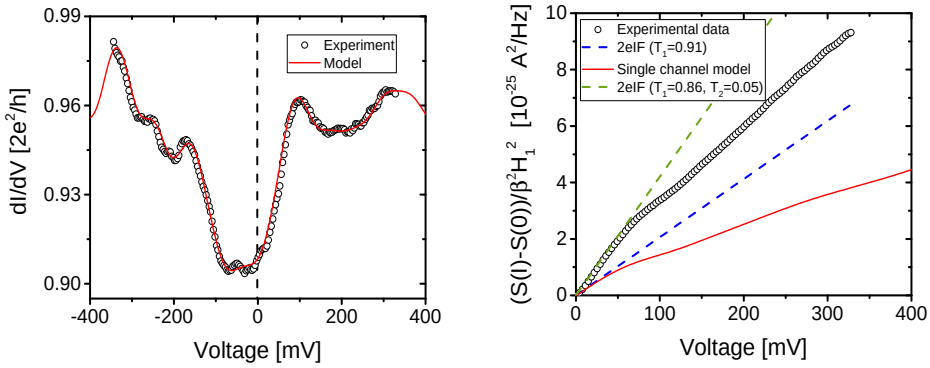

(a) Example 1: Differential conductance (left) with excess shot noise (right).

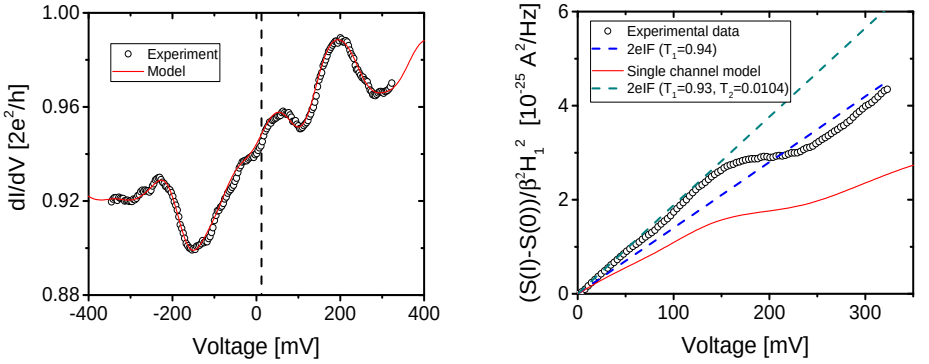

(b) Example 2: Differential conductance (left) with excess shot noise (right).

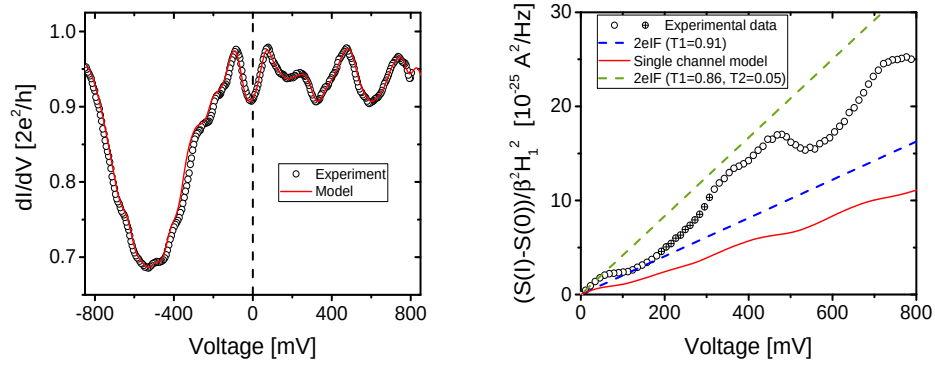

(c) Example 3: Differential conductance (left) with excess shot noise (right).

Figure 5.3: Non-linear shot-noise data: We show here three example (a),(b) and (c) of high-bias shot-noise data. The left graph in each panel shows the differential conductance of the three contacts measured and the right graph shows the corresponding shot-noise data. The experimental data is shown with black circles while the modeled $\mathrm{d}I/\mathrm{d}V$ or noise is shown by red solid curves. The points for which the noise spectra show non-white character are shown with filled circles.

level fluctuations (TLF). Thanks to our FPGA based spectrum analyzer for the noise, we can clarify this and identify any non-white occurrences (where we maintain a threshold of more than 5% deviation from the mean) in our data. This helps us in ensuring that these other noise sources are not the cause of the non-linearity in shot noise measured at high bias. Important to point out is that previous high-bias shot-noise measurements do not provide access to a spectrum to confirm the white noise character. In the noise plot of Figure 5.3 (c), there were some points with a small non-white contribution to the spectra at intermediate bias, for which the white noise part is extracted and the points are shown by filled circles in the plot. The occurrence of non-white character is attributed to two level fluctuations as explained elsewhere[13]. In the next part we will discuss the interpretation we propose for the non-linear noise based on quantum interference of electronic waves. A discussion on other possible sources of non-linearity and stability of atomic junctions at such high bias is given at the end of this chapter.

5.4 Quantum interference model

A symmetric differential conductance for positive and negative bias, could be expected for a simple point contact studied extensively in quantum transport measurements. However, experiments show that such point contacts can have very commonly a non-symmetric differential conductance. This asymmetry can be attributed to voltage dependence of transmission as will be explained below based on the Landauer formalism. Quantum interference (QI) of electronic waves due to scattering from defect sites (close to the point contact) can make the transmission voltage dependent. It is known[16–18] that such QI in the leads causes strong oscillations in the differential conductance and when the point contact transmission is near unity these oscillations become strongly suppressed. A schematic explaining this QI due to defect scattering is shown in Figure 5.4 (a). In the schematic the point contact is shown as a slit in a screen separating the two conductors left and right. Incoming electronic plane waves are shown as blue color wave-fronts. The defects are placed only on the right side of the point contact (or slit) for simplicity. The schematic shows that the electronic waves travel an additional path length on reflecting from the defect as compared to the directly transmitted wave. This creates a phase difference and the two parts of the electronic wave interfere with each other, forming constructive or destructive contributions to the current signal, depending on the position of the defects and energy of incoming beam. Compared to the analysis by[16,17] our approach differs in two important aspects: (1) We are not interested in ensemble averages but in the effects of individual defects. (2) We will be interested in the large voltage bias regime, beyond lowest-order corrections to the conductance and noise.

The first case that is considered is of a single defect at the right side of the contact where the electrons arrive after being accelerated at the contact, and add the other case later. Scattering on this defect leads to an interference term in the transmission probability. For an electron that starts from the negative-bias side with initial energy

[16] B. Ludoph et al. In: *Phys. Rev. Lett.* 82 (1999), p. 1530.
[17] B. Ludoph and J M van Ruitenbeek. In: *Physical Review B* 61 (2000), p. 2273.
[18] C. Untiedt et al. In: *Phys. Rev. B* 62 (2000), p. 9962.

E the transmission takes the form,

$$T(E,V) = T_0 + a\sin\left(2k(E,V)L + \phi\right), \tag{5.2}$$

where T_0 is the transmission that is mainly determined by the properties of the atomic contact itself, here taken to be energy and voltage independent. The amplitude a depends on the distance of the defect and the scattering probability. This amplitude decreases with the distance L between the defect and the contact as L^{-4}, as result of the solid angle under which the defect is seen from the contact and, after scattering on the return path, the solid angle under which the contact is seen from the defect position. Along its path the scattering partial wave accumulates a phase $2k(E,V)L$ with respect to the partial wave that is directly transmitted, plus a constant phase ϕ is added[18], which depends on the details of the scattering process. This makes the total transmission both energy and voltage dependent $T(E,V)$.

The wavenumber $k(E,V)$ depends on the total energy (E) of the incoming electron and the voltage drop (V) experienced at the point contact. Due to the acceleration of the electron at the contact site the wave-number of electrons after the contact will be,

$$k(E,V) = \frac{\sqrt{2m(E+eV/2)}}{\hbar} \tag{5.3}$$

So, for multiple defects the transmission takes the form:

$$T(E,V) = T_0 + \sum_{p=0}^{N_d} a_p \sin\left(2L_p \frac{\sqrt{2m(E+eV/2)}}{\hbar} + \phi_p\right) = T(E+eV/2) = T(\zeta) \tag{5.4}$$

where N_d is the number of defect sites. As the energy (E) and applied bias (V) enter in the above transmission picture only in the combination $E + eV/2$, we can write the total transmission as a function of a single variable: $\zeta = E + eV/2$. The above total transmission is written for a single channel; for multiple channels one has to use a second index n with transmission of n^{th} channel as $T_n(\zeta)$. As the transmission enters as $T(1-T)$, this energy and voltage dependent transmission could cause strong non-linearities in the shot noise. Before going ahead we discuss the assumptions made in the model. (1) We will assume for simplicity that only a single channel is taking part in transport. (2) We assume zero temperature, which helps us in getting rid of the Fermi functions from the integrals shown in the later part. This is a reasonable assumption as the experiments shown here are done at liquid helium temperatures, and we work in the regime $eV \gg k_B T$. (3) We assume that all the voltage drops over the point contact and not over the defects. (4) We leave out any intrinsic energy dependence of the transmission for the metallic point contacts[19]. (5) We take the waves to be reflected only once from the defect sites. More than one reflection will reduce the amplitude of the wave significantly. (6) We assume the transmission is entirely described by elastic processes. Inelastic scattering on vibration modes of the contact are briefly discussed below.

Under these assumptions the total transmission of the system can be taken as given in equation 5.4 due to QI of electronic waves. Because this transmission is both

[19] Mads Brandbyge et al. In: *Phys. Rev. B* 60 (1999), p. 17064.

energy and voltage dependent, we have to use the generalized non-linear Landauer's expression for time averaged current $\langle I \rangle (V)$ and noise $S_I(V)$ for spin degenerate systems[6–8,20,21].

$$\langle I \rangle (V) = 2\frac{e}{h} \sum_{n=1}^{N} \int_{-\infty}^{+\infty} \mathrm{d}E\, T_n(E,V)[f_L - f_R] \tag{5.5}$$

$$\begin{aligned} S_I = 4\frac{e^2}{h} \sum_{n=1}^{N} \int_{-\infty}^{+\infty} \mathrm{d}E \{ & T_n(E,V)[f_L(1-f_L) + f_R(1-f_R)] \\ & + T_n(E,V)(1-T_n(E,V))[f_L - f_R]^2 \} \end{aligned} \tag{5.6}$$

As we make the assumption that the approximation of zero temperature the Fermi functions f_L and f_R can be taken as Heaviside functions. On using the Leibniz integration rule one can write an expression for the differential conductance G_{diff} or $\frac{\mathrm{d}\langle I \rangle}{\mathrm{d}V}$[22,23] starting from equation 5.5,

$$\frac{\mathrm{d}\langle I \rangle}{\mathrm{d}V} = 2\frac{e}{h} \sum_{n=1}^{N} \left\{ \frac{e}{2} T_n(E_F + \frac{eV}{2}, V) + \frac{e}{2} T_n(E_F - \frac{eV}{2}, V) + \int_{E_F - \frac{eV}{2}}^{E_F + \frac{eV}{2}} \frac{\partial T_n(E,V)}{\partial V} \mathrm{d}E \right\} \tag{5.7}$$

which for a single channel becomes:

$$= 2\frac{e^2}{h} \left\{ \frac{T_H + T_L}{2} + \frac{1}{e} \int_{E_F - \frac{eV}{2}}^{E_F + \frac{eV}{2}} \frac{\partial T}{\partial V} \mathrm{d}E \right\} \tag{5.8}$$

where, $T_H = T(E_F + \frac{eV}{2}, V) = T(E_F + eV)$ and $T_L = T(E_F - \frac{eV}{2}, V) = T(E_F)$. The meaning of T_H and T_L is explained in the Figure 5.4 (b). Here a simple model curve $T(\zeta)$ for a single channel taking only one sine term in equation 5.4 is plotted against energy ζ. As a bias voltage is applied, an energy window of width eV centered at $E_F + eV/2$ is opened. T_H and T_L are the values of the transmission at the 'High' and 'Low' side of the window as shown in the Figure 5.4(b). If there is no voltage dependence of the transmission (i.e., $\frac{\partial T}{\partial V} = 0$), then only the width of the energy window changes but the center will stay at $\zeta - E_F = 0$ and the total conductance will be an arithmetic mean of the T_H and T_L. Moreover, for the case of only energy dependence, one needs to know the $T(E)$ over a window of size eV from $E_F - eV/2$ to $E_F + eV/2$. On the contrary, for the case of both energy and voltage dependence, transmission has to be known over a window of width 2 eV from $\zeta = -eV$ to $\zeta = +eV$ to know the complete differential conductance and shot noise from negative to positive bias. Further, it is important to note that if the transmission is constant or only energy dependent, then from equation 5.7, the $\mathrm{d}I/\mathrm{d}V$ will be symmetric

[20] Nicolás Agraït et al. In: *Physics Reports* 377 (2003), p. 81.
[21] Juan Carlos Cuevas and Elke Scheer. Molecular electronics : an introduction to theory and experiment. New Jersey [u.a.] : World Scientific, 2010.
[22] Eleuterio Castao and George Kirczenow. In: *Phys. Rev. B* 41 (1990), p. 3874.
[23] Gaibo Zhang et al. In: *Journal of Physical Chemistry C* 119 (2015), p. 6254.

for the positive and negative bias. Any asymmetry in $\mathrm{d}I/\mathrm{d}V$ is arising from the voltage dependence of the transmission. The asymmetry in $\mathrm{d}I/\mathrm{d}V$ is also attributed to asymmetric potential drop between the left and right reservoir[24], which could be due to potential drop over defects which are randomly placed.

Because the last term in the expression for the differential conductance given in equation 5.8 is an integration over only energy (E), we can write $\frac{\partial T}{\partial V}\mathrm{d}E = \frac{\mathrm{d}T}{\mathrm{d}\zeta}\frac{\partial \zeta}{\partial V}\mathrm{d}\zeta = \frac{1}{2}e\mathrm{d}T(\zeta)$.

$$\Rightarrow \int_{E_\mathrm{F}-\frac{eV}{2}}^{E_\mathrm{F}+\frac{eV}{2}} \frac{\partial T}{\partial V}\mathrm{d}E = \frac{1}{2}e\int_{E_\mathrm{F}}^{E_\mathrm{F}+eV} \mathrm{d}T(\zeta) = \frac{1}{2}e(T_\mathrm{H}-T_\mathrm{L}) \tag{5.9}$$

From equation 5.8 the differential conductance can be written as:

$$\Rightarrow \frac{\mathrm{d}\langle I\rangle}{\mathrm{d}V} = 2\frac{e^2}{h}\left\{\frac{T_\mathrm{H}+T_\mathrm{L}}{2}+\frac{T_\mathrm{H}-T_\mathrm{L}}{2}\right\} = 2\frac{e^2}{h}T_\mathrm{H} \tag{5.10}$$

If we include scattering over defects present both before (left) and after (right) the point contact, the expression for differential conductance over all defects will be:

$$\begin{aligned}\frac{\mathrm{d}\langle I\rangle}{\mathrm{d}V} = \frac{2e^2}{h}\Bigg[T_0 &+ \sum_{p=0}^{N_r} a_p \sin\left(2L_p\frac{\sqrt{2m(E_\mathrm{F}+eV)}}{\hbar}+\phi_p\right)\\ &+ \sum_{q=0}^{N_l} a_q \sin\left(2L_q\frac{\sqrt{2m(E_\mathrm{F}-eV)}}{\hbar}+\phi_q\right)\Bigg]\end{aligned} \tag{5.11}$$

Where N_l and N_r are the numbers of defects on the left and right of the point contact, respectively. As long as $eV \ll E_\mathrm{F}$ the sine terms in the summation for the left and right defects have the same dependence on V, so a defect sitting on the left will give the same frequency dependence (within a constant phase factor) as a defect at the same radial distance on the right. In our model we will use the expression with defects sitting only on one side of the point contact. As we are interested in studying non-linear shot noise, we want to also derive an expression for differential shot noise $\frac{\mathrm{d}S_\mathrm{I}}{\mathrm{d}V}$. We define a function $Z(E,V) = T(E,V)(1-T(E,V))$ and making again the zero temperature and single channel assumption, we rewrite equation 5.6 as :

$$S_\mathrm{I} = 4\frac{e^2}{h}\int_{E_\mathrm{F}-\frac{eV}{2}}^{E_\mathrm{F}+\frac{eV}{2}} \mathrm{d}E\,\{T(E,V)(1-T(E,V))\} = 4\frac{e^2}{h}\int_{E_\mathrm{F}-\frac{eV}{2}}^{E_\mathrm{F}+\frac{eV}{2}} Z(E,V)\mathrm{d}E \tag{5.12}$$

This expression for noise has the same form as the equation 5.5 for current. Without the need for repeating the exercise we did above for differential conductance we can immediately write the differential shot noise as:

$$\frac{\mathrm{d}S_\mathrm{I}}{\mathrm{d}V} = 4\frac{e^3}{h}Z_\mathrm{H} = 4\frac{e^3}{h}T_\mathrm{H}(1-T_\mathrm{H}) \tag{5.13}$$

[24] A. García-Martín et al. In: *Phys. Rev. B* 62 (2000), p. 11139.

It is important to note the difference between the above expressions for conductance and noise with those for the low-bias linear regime, where we assume constant transmission. In the linear regime, the differential conductance is given by the Landauer formula i. e. $G(E_F) = 2\frac{e^2}{h}T(E_F)$ and shot noise is given by $S_I = 2eIF = 2eVG(E_F)F$ with the Fano factor $F = 1 - T(E_F)$. This gives the noise for the linear regime constant transmission case as $S_I = 4\frac{e^3}{h}VT(E_F)(1 - T(E_F))$, which, of course, gives a linear increase in noise with bias, with complete suppression of noise at transmission close to $T(E_F) = 0$ and 1. In the quantum interference picture for the non-linear regime, the differential conductance (equation 5.10) has close similarity with the linear regime formula, with the difference that now the transmission should be evaluated at the high-bias end of the energy window. The expression for shot noise is however quite different. Equation 5.13 shows the expression for $\frac{dS_I}{dV}$ and not S_I. So, here as the transmission will go to 1, the noise is not going to be zero, but rather the slope of the noise will be zero and we will see a plateau appearing in the noise curve.

We would like to stress that the subtle similarities with the linear regime expressions for noise and differential conductance are only valid in the special case of single-channel quantum interference. To be more precise, they are valid in the case where the non-linear transmission is of the form $T(E, V) = T(E + eV/2)$. In a later section 5.5, we analyze a transmission of more general form $T(\alpha E + \gamma eV)$ and we have studied mathematically its effects on shot noise and differential conductance.

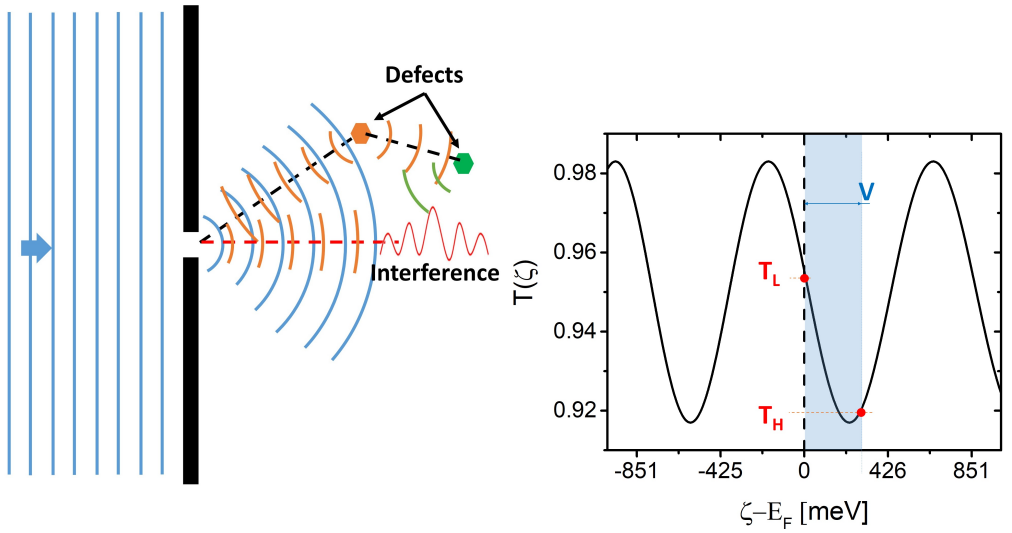

(a) (b)

Figure 5.4: (a) Model based on quantum interference of electronic waves due to scattering from defects in the leads. The point contact is represented as a single slit with defects only shown on the right side. Multiple reflections as shown for the green defect are not taken into account (b) Example of a model transmission for a single defect shown to explain the meaning of T_H and T_L.

5.4.1 Extraction of the voltage and energy dependent transmission

For the single channel quantum interference model, we can calculate back the transmission function given in equation 5.4. For comparing with the experimental differential conductance data we need to include more than just a single sine term in the sum in equation 5.4. For obtaining the unknown variables (a_p, L_p, ϕ_p) from experimental data we extract the different Fourier components constituting the measured differential conductance, an example is shown in Figure 5.5 (a). Next, by using one sine term at a time in T(E,V) (equation 5.4) we calculate the differential conductance from the model and match it with one of the Fourier components of the measured data. From this match we obtain the values of a_p, L_p and ϕ_p. The more Fourier components we use the more sine terms in the sum in the expression for T(E,V) we could compute. Once we have obtained the set of a_p, L_p and ϕ_p values we combine the sine terms from which we can calculate the complete T(E,V) surface shown in Figure 5.5 (b).

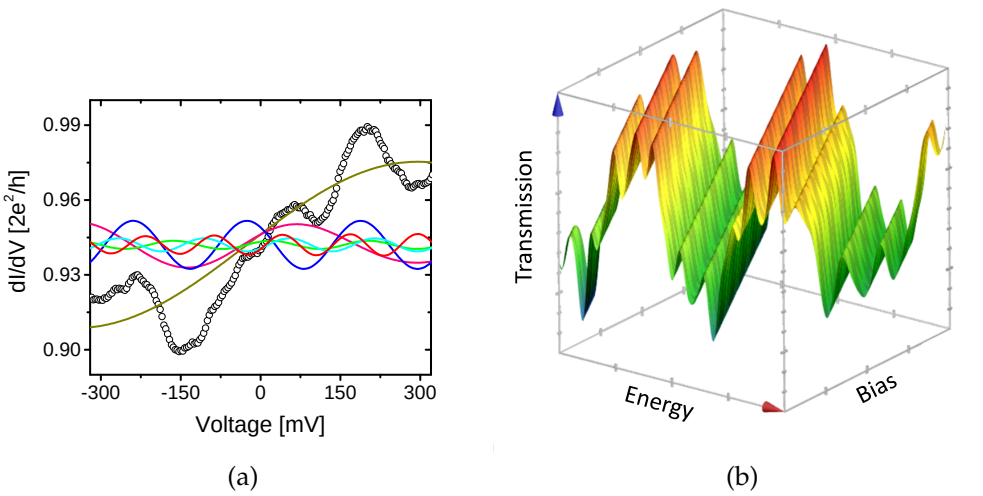

(a) (b)

Figure 5.5: (a) First 6 harmonics of the differential conductance associated to nearest six defects. (b) Complete T(E,V) surface extracted from the experimental data within the single channel quantum interference picture.

The complete function T(E,V) permits calculating also other properties, and specifically the shot noise for the same contact. However, by virtue of the analysis given above we can follow a simpler procedure.

5.4.2 Analysis of the experimental data

We start by taking a single-channel linear-regime assumption and show the noise ($S_I = 2eI(1-T)$) with the blue dashed lines for all the three examples in Figure 5.3, where we have obtained the transmission from the measured differential conductance ($T = G[G_0]$) at zero bias for the three data sets. From here we see that the experimental data suggest the presence of a second channel whose transmission at zero bias can be extracted by fitting the measured noise data with a straight line at low bias (see

Appendix C.2). This is shown by the green dashed lines in Figure 5.3 for the three examples and the extracted zero-bias transmission for the second channel (T_2) is also mentioned. Although, we know from this that the three examples we study here are not correctly described by just a single channel, we will first try to use our simple single channel model to understand the measured non-linearity in the shot noise.

Using equation 5.10, we can write $T_{\mathrm{H}} = \frac{h}{2e^2}\mathrm{d}I/\mathrm{d}V = G[G_0]$. This, $G[G_0]$ is the differential conductance in units of $G_0 = 2\frac{e^2}{h}$ and we measure this in experiments. From here we can rewrite equation 5.13 for the differential shot noise as:

$$\frac{\mathrm{d}S_{\mathrm{I}}}{\mathrm{d}V} = 4\frac{e^3}{h}G(1-G) \tag{5.14}$$

Next, we input the experimentally measured conductance values in equation 5.14 and integrate it over the whole bias range. The modeled noise thus obtained is shown with solid red curves in Figure 5.3 in the three examples. In all three examples, the noise reproduces qualitatively the non-linearities in the experimental data. This is a surprisingly good match considering the assumptions made in the model.

In example 1 and 2, the model explains the kink and the step structure arising in the noise as an intrinsic property of the contact depending on the position of the defect sites. In example 3 also the modeled noise explains the occurrence of rather complicated non-linearity in the measured shot noise, although the decrease of shot noise with voltage bias observed in the experiments cannot be reproduced. This can also be seen from the expression of $\mathrm{d}S_{\mathrm{I}}/\mathrm{d}V$ shown in equation 5.13, which shows that the $\mathrm{d}S_{\mathrm{I}}/\mathrm{d}V$ can never be negative for the current choice of T(E,V). Important to note is that our model is purely elastic, there are no inelastic effects included and no free parameters used for tweaking the shape of the modeled noise. We are showing here that pure elastic scattering can give large non-linearities in shot noise and we can measure these precisely in our experiments.

The quantitative mismatch and fact that our model does not follow the strong non-linearities such as the negative differential shot noise observed in the experiments could be attributed to two main reasons. (1) The inelastic effects: these are not included in our simple model, but they must be playing a role at such high bias. We know for contacts with conductance close to 1 G_0, the conductance decreases due to inelastic backscattering of electrons. Such effects are not included in the model. (2) The intrinsic energy dependence of the transmission of the point contact itself is ignored (T_0 is taken to be constant in equation 5.4). In reality T_0 can be dependent on both energy and voltage as can be seen in the article by Brandbyge *et al*.[19]. (3) As the transmission enters in the form $T(1-T)$ in the shot noise, which makes the noise for a channel with T close to 1 very small and even a small contribution from a second channel with transmission close to zero could become comparable, which is not included in our model. Simply adding a constant second channel will add to the noise but will also smooth out the non-linearities in our model (see Appendix C.2). Ideally, we need to include the second channel effect in the quantum interference model, but this goes at the expense of adding many free parameters.

For a complete match one has to find the complete expression for $T(E,V)$ including the inelastic effects, which is not trivial to extract from just shot noise and differential conductance data and further analysis awaits input from theory.

5.5 More general energy and voltage dependent transmission functions

As a formal exercise we discuss a more generalized expression for $T(E,V)$ where we take $T(E,V) = T(\alpha E + \gamma eV) = T(E + \beta eV)$ as opposed to $T(E + eV/2)$ coming from the QI picture. We show here that , despite the fact that the transmission is bounded in the range [0,1] and is a smooth function, it can lead to situations where the shot noise decrease with bias and differential conductance for a single channel becomes larger than 1 or smaller than 0. Note that at this point we do not attempt to associate the values for β with specific physical processes (other than for $\beta = \pm\frac{1}{2}$). Negative differential conductance has been long known, for example in two-dimensional electron gas (2DEG)[25], which results from QI, same as for the differential conductance of our atomic contacts. However, conductance of a single channel larger that 1 (super-Landauer single channel, SLSC) has not been known nor has a decrease of shot noise with bias or negative differential shot noise (NDSN) in ballistic point contacts as shown in Fig 5.3 (c).

Again we start by writing the function T(E,V) in terms of a single variable $\zeta = E + \beta eV$. Next, $\frac{\partial T}{\partial V}$ can be written as :

$$\frac{\partial T}{\partial V} = \frac{\partial T}{\partial \zeta}\frac{\partial \zeta}{\partial V} = \beta e \frac{\partial T}{\partial \zeta} \tag{5.15}$$

From here we can write an expression for the differential conductance,

$$\frac{\mathrm{d}\langle I\rangle}{\mathrm{d}V} = \frac{2e^2}{h}\left\{\tfrac{1}{2}(T_\mathrm{H} + T_\mathrm{L}) + \beta(T_\mathrm{H} - T_\mathrm{L})\right\} = \frac{e^2}{h}\left[(2\beta+1)T_\mathrm{H} - (2\beta-1)T_\mathrm{L}\right] \tag{5.16}$$

Moreover, from equation 5.12 we know that the time averaged current $\langle I\rangle\,(V)$ and $S_\mathrm{I}(V)$ share the same functional form, so without redoing the above calculation, we can write the form for differential shot noise $\mathrm{d}S_\mathrm{I}/\mathrm{d}V$ as:

$$\frac{\mathrm{d}S_\mathrm{I}}{\mathrm{d}V} = \frac{2e^3}{h}\left[(2\beta+1)Z_\mathrm{H} - (2\beta-1)Z_\mathrm{L}\right] \tag{5.17}$$

where, $Z_\mathrm{H} = T_\mathrm{H}(1 - T_\mathrm{H})$ and $Z_\mathrm{L} = T_\mathrm{L}(1 - T_\mathrm{L})$.

The main properties of the above equations are summarized in Figure 5.6 (a). When $T_\mathrm{H} < \frac{2\beta-1}{2\beta+1}T_\mathrm{L}$ then the single transmission channel shows negative differential conductance (NDC). This condition is shown as the blue triangular region on the left. When $(2\beta+1)T_\mathrm{H} - (2\beta-1)T_\mathrm{L} > 2$ the single transmission channel will have conductance larger than 1 G_0. This upsets the existing notion (correct in the linear regime) that a single channel can have at maximum one quantum of conductance. In the non-linear regime for transmission of the form $T(E + \beta eV)$ discussed here, equation 5.16 shows that the maximum conductance for the single channel can be as large as 1.5 G_0. We call this state super Landauer single channel (SLSC) and it is shown in Figure 5.6 (a) as the blue shaded triangular region on the right. From the relation of differential shot noise (equation 5.17) one can see that for $(2\beta+1)Z_\mathrm{H} < (2\beta-1)Z_\mathrm{L}$ the shot noise will decrease with increase in bias and we enter a regime called negative differential shot noise (NDSN). This is shown as the red shaded region

[25] R. J. Brown et al. In: *Journal of Physics: Condensed Matter* 1 (1989), p. 6285.

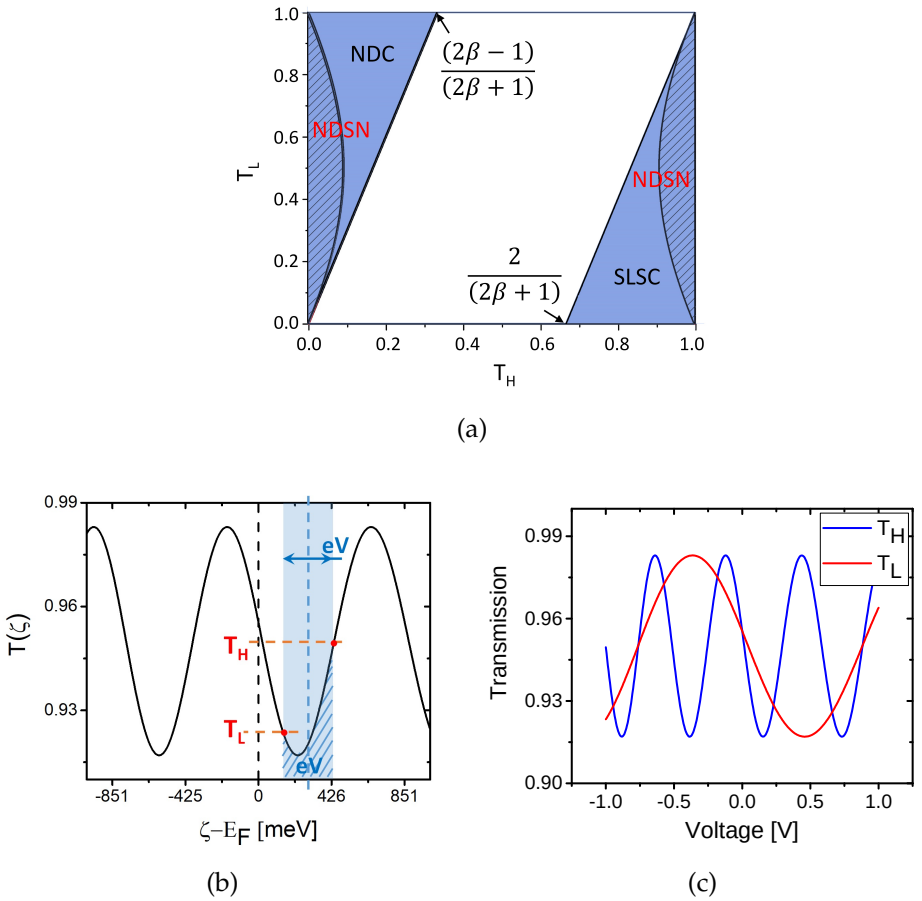

Figure 5.6: (a) Model based on a more general energy and voltage dependent transmission functions given by $T(E+\beta eV)$. The blue triangular region on the left is where the differential conductance is negative (NDC), while the similar blue region on the right shows the super Landauer single channel (SLSC) region where the differential conductance for a single channel exceeds 1 G_0. The shaded red regions on the left and right are where the differential shot noise is negative (NDSN). (b) Example of a model transmission for $\beta = 1$ shown to explain the meaning of T_H and T_L. (c) The T_H and T_L profiles extracted from the above transmission.

on the left and right. From the figure we also see that NDSN occurs when either NDC or SLSC is present but the presence of NDC and SLSC does not always means that we will have NDSE. To illustrate further, we present here an example with the single channel transmission at $\beta = 1$ shown in the Figure 5.6 (b). The differential conductance calculated from this is shown in Figure 5.7 (a) where we see that the dI/dV crosses 1 G_0 at around 450 mV. Figure 5.7(b) shows the corresponding noise where we see that the noise stagnates and starts to decrease around the same bias when the differential conductance is larger than 1 G_0.

Here we see that the transmission T(E,V) could take forms which are mathemat-

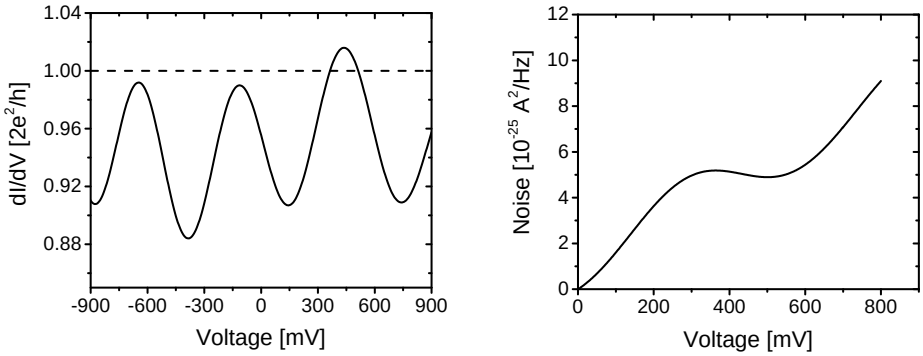

(a) (b)

Figure 5.7: (a) Differential conductance calculated for the transmission shown in Figure 5.6 with conductance crossing 1 G_0 (SLSC). (b) The noise calculated for the same model shows NDSN behavior in the regime for which the dI/dV is larger than 1 G_0.

ically allowed and lead to exotic states like NDC, NDSN and SLSC. We are aware that we are not providing a physical basis for values of β other than $\beta = \pm 1/2$ which is associated with the quantum interference of electronic waves discussed in this chapter. The question whether other values of β are possible is a part of a broader question which possible functions $T(E, V)$ are allowed.

5.6 Discussion

In the previous section we have offered an interpretation for the non-linear dependence of shot noise on the applied bias. We have seen that, qualitatively, the effects are related to those in the differential conductance, and these are likely due to quantum interference as a result of electrons scattering from defects near the contact. For a quantitative explanation more elaborate models are required, and the observed negative differential noise is particularly exotic. High-bias shot-noise measurements have been reported earlier for Au atomic contacts up to 300 mV in room temperature[14] and 250 mV at low temperatures[15]. These measurements were performed using a high bandwidth radio-frequency (rf) technique, where only the integrated noise is detected by a power detector. The reported non-linearity in shot noise was shown only as a rise in noise power. In case of the room temperature measurements[14] the non-linear increase in shot noise was attributed to either electron-phonon interaction or local heating of the electronic fluid which crosses the ballistic junction. At low temperature[15] the non-linear rise is explained using the linear regime Landuaer formalism relations, which in general should not be applicable at high bias as explained earlier. Also an occurrence of decrease in shot noise with bias has been reported[26] on a n-GaAs MESFET system where due to correlated resonant tunneling (which

[26] S. S. Safonov et al. In: *Phys. Rev. Lett.* 91 (2003), p. 136801.

involves two interacting resonant states) first an enhancement in the shot noise over the Poisson value ($2eI$) occurs and then a decrease in shot noise with bias. Other possible explanations proposed for non-linearity in shot noise[27] are bias-dependent channel mixing and nonequilibrium phonon back-action. A non-equilibrium phonon distribution[11] could develop but as a result of the strong coupling to the phonon bath in the Au leads, the non-equilibrium is expected to remain small. Such effects are more important in systems where the vibrons of the system are weakly coupled to the phonon bath of the leads. On the theory side, Lesovik and Loosen[28] have shown that the excess noise ($S(I) - S(0)$) could even become negative for a sharp peak in transmission, close to zero bias, whose width is much smaller than $k_B T$. This is a very rarely occurring possibility and has not been found yet in the experiments.

Stability and heating of atomic point contacts at such high bias can also be a concern and has been studied earlier as well[29], where it was reported that Au atomic contacts could even sustain up to 2 V and more than 150 μA current. Using a semi-classical approach[20,30,31] , it has been shown that in the ballistic regime, where the size of the contact is much smaller than the mean free path, the heat carried by electrons under an applied bias is dissipated far away in the banks via scattering with phonons. As a result, even at such high bias, the effect of heating on noise and G_{diff} can be ignored, as the electronic temperature in the vicinity of ballistic point contact does not rise much. We measured the global heating effect in our samples by replacing the Au point contact with a standard film resistor of 13 kΩ (close to 1 G_0) and recording the noise. From the noise measurement we conclude that the rise in effective temperature for up to 1 V bias over the 13 kΩ resistor, is around 0.075 K which is equivalent to 0.23 nV/$\sqrt{\text{Hz}}$ in thermal noise.

5.7 Conclusion and outlook

In conclusion, we have performed shot-noise measurements over Au single atom point contacts in the non-linear regime, even up to 800 mV bias as shown in the 3$^{\text{rd}}$ example in Figure 5.3. These shot noise data show highly non-linear behavior with applied bias, which has no specific trend and which is different for every different contact. We have shown that these non-linearities arise due to quantum interference of electronic waves which take multiple paths due to elastic scattering on the defects present in the leads close to the point contact. This makes the transmission probability of the contact energy and voltage dependent, which means usual assumptions based on the linear regime breakdown. We can qualitatively explain the main features in the measured non-linearity but there could also be other energy and voltage dependent effects present, due to the intrinsic transmission of the point contact itself, the effect of other channels and the voltage drop over the defect sites. Any inelastic effects, including non-equilibrium phonon back action and back-scattering of electrons which could lower the junction conductance is also not included in the model. We have

[27] Loah A. Stevens et al. In: *Journal of Physics: Condensed Matter* 28 (2016), p. 495303.
[28] Gordey B. Lesovik and Roland Loosen. In: *Zeitschrift für Physik B Condensed Matter* 91 (1993), p. 531.
[29] S. K. Nielsen et al. In: *Phys. Rev. Lett.* 89 (2002), p. 066804.
[30] Yu V. Sharvin. In: *J. Exptl. Theoret. Phys. (U.S.S.R.)* 48 (1965), p. 655.
[31] A. G. M. Jansen et al. In: *Journal of Physics C: Solid State Physics* 13 (1980), p. 6073.

presented experimental data where the non-linearity is such that the shot noise even decreases with increase in bias (NDSN). We argue that this is not permitted within the standard description of elastic scattering, but we have discussed mathematically a possibility that certain forms of T(E,V) could even lead to more exotic states like NDC and SLSC. The results presented in this chapter suggest that if the position of defects in the vicinity of the point contact can be controlled, then by exploiting the quantum interference of electronic waves, one could design the transmission at will and achieve desired properties in conductance and noise. In a metallic point contact it is not easy to control the position of defects, but in a pre-designed molecular system and mesoscopic systems like 2DEG[32] this may be feasible.

[32] M. A. Topinka et al. In: *Science* 289 (2000), p. 2323.